Formation and evolution mechanisms of plasmon-induced transparency in MDM waveguide with two stub resonators

Guangtao Cao,[1, 2] Hongjian Li,[1, 2,*] Shiping Zhan,[1] Haiqing Xu,[1] Zhimin Liu,[1] Zhihui He,[1] and Yun Wang[1]

[1]*College of Physics and Electronics, Central South University, Changsha 410083, China*
[2]*College of Materials Science and Engineering, Central South University, Changsha 410083, China*
[*]*lihj398@yahoo.com.cn*

残端，掐灭

Abstract: We demonstrate the realization of plasmonic analog of electromagnetically induced transparency (EIT) in a system composing of two stub resonators side-coupled to metal-dielectric-metal (MDM) waveguide. Based on the coupled mode theory (CMT) and Fabry-Perot (FP) model, respectively, the formation and evolution mechanisms of plasmon-induced transparency by direct and indirect couplings are exactly analyzed. For the direct coupling between the two stub resonators, the FWHM and group index of transparent window to the inter-space are more sensitive than to the width of one cut, and the high group index of up to 60 can be achieved. For the indirect coupling, the formation of transparency window is determined by the resonance detuning, but the evolution of transparency is mainly attributed to the change of coupling distance. The consistence between the analytical solution and finite-difference time-domain (FDTD) simulations verifies the feasibility of the plasmon-induced transparency system. It is also interesting to notice that the scheme is easy to be fabricated and may pave the way to highly integrated optical circuits.

OCIS codes: (240.6680) Surface plasmons; (230.7370) Waveguides; (130.3120) Integrated optics devices.

References and links

1. K. J. Boller, A. Imamolu, and S. E. Harris, "Observation of electromagnetically induced transparency," Phys. Rev. Lett. **66**(20), 2593–2596 (1991).
2. Y. Zhang, K. Hayasaka, and K. Kasai, "Conditional transfer of quantum correlation in the intensity of twin beams," Phys. Rev. A **71**(6), 062341 (2005).
3. S. Harris and L. Hau, "Nonlinear optics at low light levels," Phys. Rev. Lett. **82**(23), 4611–4614 (1999).
4. H. Gersen, T. J. Karle, R. J. Engelen, W. Bogaerts, J. P. Korterik, N. F. van Hulst, T. F. Krauss, and L. Kuipers, "Real-space observation of ultraslow light in photonic crystal waveguides," Phys. Rev. Lett. **94**(7), 073903 (2005).
5. L. V. Hau, S. E. Harris, Z. Dutton, and C. H. Behroozi, "Light speed reduction to 17 metres per second in an ultracold atomic gas," Nature **397**(6720), 594–598 (1999).
6. Q. Xu, S. Sandhu, M. L. Povinelli, J. Shakya, S. Fan, and M. Lipson, "Experimental realization of an on-chip all-optical analogue to electromagnetically induced transparency," Phys. Rev. Lett. **96**(12), 123901 (2006).
7. X. Yang, M. Yu, D. L. Kwong, and C. W. Wong, "All-optical analog to electromagnetically induced transparency in multiple coupled photonic crystal cavities," Phys. Rev. Lett. **102**(17), 173902 (2009).
8. K. Totsuka, N. Kobayashi, and M. Tomita, "Slow light in coupled-resonator-induced transparency," Phys. Rev. Lett. **98**(21), 213904 (2007).
9. Y. F. Xiao, X. B. Zou, W. Jiang, Y. L. Chen, and G. C. Guo, "Analog to multiple electromagnetically induced transparency in all-optical drop-filter systems," Phys. Rev. A **75**(6), 063833 (2007).
10. T. W. Ebbesen, C. Genet, and S. I. Bozhevolnyi, "Surface-plasmon circuitry," Phys. Today **61**(5), 44–50 (2008).
11. D. K. Gramotnev and S. I. Bozhevolnyi, "Plasmonics beyond the diffraction limit," Nat. Photonics **4**(2), 83–91 (2010).
12. Y. Huang, C. Min, and G. Veronis, "Subwavelength slow-light waveguides based on a plasmonic analogue of electromagnetically induced transparency," Appl. Phys. Lett. **99**(14), 143117 (2011).
13. L. Yang, C. G. Min, and G. Veronis, "Guided subwavelength slow-light mode supported by a plasmonic waveguide system," Opt. Lett. **35**(24), 4184–4186 (2010).

#179233 - $15.00 USD Received 6 Nov 2012; revised 15 Mar 2013; accepted 26 Mar 2013; published 8 Apr 2013

14. Y. Zhang, S. Darmawan, L. Y. M. Tobing, T. Mei, and D. H. Zhang, "Coupled resonator-induced transparency in ring-bus-ring Mach-Zehnder interferometer," J. Opt. Soc. Am. B **28**(1), 28–36 (2011).
15. Z. H. Han and S. I. Bozhevolnyi, "Plasmon-induced transparency with detuned ultracompact Fabry-Perot resonators in integrated plasmonic devices," Opt. Express **19**(4), 3251–3257 (2011).
16. G. X. Wang, H. Lu, and X. M. Liu, "Dispersionless slow light in MIM waveguide based on a plasmonic analogue of electromagnetically induced transparency," Opt. Express **20**(19), 20902–20907 (2012).
17. H. Lu, X. M. Liu, and D. Mao, "Plasmonic analog of electromagnetically induced transparency in multi-nanoresonator-coupled waveguide systems," Phys. Rev. A **85**(5), 053803 (2012).
18. H. Lu, X. M. Liu, D. Mao, Y. K. Gong, and G. X. Wang, "Induced transparency in nanoscale plasmonic resonator systems," Opt. Lett. **36**(16), 3233–3235 (2011).
19. X. J. Piao, S. Yu, S. Koo, K. H. Lee, and N. Park, "Fano-type spectral asymmetry and its control for plasmonic metal-insulator-metal stub structures," Opt. Express **19**(11), 10907–10912 (2011).
20. Y. H. Guo, L. S. Yan, W. Pan, B. Luo, K. H. Wen, Z. Guo, and X. G. Luo, "Electromagnetically induced transparency (EIT)-like transmission in side-coupled complementary split-ring resonators," Opt. Express **20**(22), 24348–24355 (2012).
21. R. D. Kekatpure, E. S. Barnard, W. Cai, and M. L. Brongersma, "Phase-coupled plasmon-induced transparency," Phys. Rev. Lett. **104**(24), 243902 (2010).
22. E. N. Economou, "Surface Plasmons in Thin Films," Phys. Rev. **182**(2), 539–554 (1969).
23. E. D. Palik, *Handbook of Optical Constants in Solids* (Academic, 1982).
24. H. A. Haus and W. P. Huang, "Coupled-mode theory," Proc. IEEE **79**(10), 1505–1518 (1991).
25. H. A. Haus, *Waves and fields in optoelectronics* (Prentice-Hall, New Jersey, 1984).
26. T. Baba, "Slow light in photonic crystal," Nat. Photonics **2**(8), 465–473 (2008).

1. Introduction

Electromagnetically induced transparency (EIT) observed in atomic media results from a coherent interaction between the atomic levels and the applied optical fields [1]. EIT promises a variety of potential applications such as slow light propagation, transfer of quantum correlation, and nonlinear optical process [2–5]. The demanding experimental conditions required to observe the EIT effect hinder its practical application, which catalyzes an ongoing search for classical systems mimicking EIT. In recent years, theoretical analysis and experimental observations have revealed that the EIT-like phenomena can also occur in dielectric photonic resonator systems, which is known as coupled-resonator induced transparency [6–9].

It is noteworthy that controlling light on a small scale is very essential for highly integrated optics. Surface plasmon polaritons (SPPs) propagating along the metal-dielectric interface can be well confined by ultrasmall metal structures and break the diffraction limit [10,11]. Among the different plasmonic devices, metal-dielectric-metal (MDM) plasmonic waveguides are of particular interest, because they support modes with deep wavelength scale and an acceptable length for SPPs. Based on the unique feature of MDM waveguides, the plasmonic analogue of EIT observed in nanoscale plamonic resonator systems was theoretically predicted and experimentally demonstrated in recent researches [12–20]. Veronis et al. introduced systems composing of a periodic array of metal-dielectric-metal (MDM) stub resonators side coupled to MDM waveguide, and showed that there is a trade off between the slowdown factor and the propagation length of the supported optical mode [12,13]. The on-chip plasmonic analogue of EIT was realized by detuned Fabry-Perot (FP) resonators aperture-side-coupled to a MDM waveguide [15]. In [17], Lu et al. demonstrated an analog of EIT and multiple induced-transparency peaks in plasmonic systems consisting of multiple cascaded nanodisk resonators, aperture-side-coupled to MDM bus waveguides. However, very few comprehensive studies have been performed on plasmon-induced transparency in MDM waveguide with two stub resonators.

In this paper, we investigate the EIT-like spectral responses and slow-light effects in plasmonic system composed of two stub resonators side-coupled to MDM bus waveguides. The system is easy to be realized and different from the configuration reported in [15,17,21]. In particular, the formation and evolution mechanisms of the transparency response induced by direct coupling and indirect coupling have been accurately analyzed through the CMT and FP model, respectively.

#179233 - $15.00 USD Received 6 Nov 2012; revised 15 Mar 2013; accepted 26 Mar 2013; published 8 Apr 2013

2. Theoretical analysis and discussion of MDM waveguide with one stub resonator

Figure 1(a) shows the dispersion curves for TM mode [22] in MDM waveguide with width h = 100 nm. The blue curve is for the real part of the effective index of SPPs, and the green curve is for the imaginary part. The inset in Fig. 1(a) is MDM waveguide structure with width h. The medium of the slit is assumed to be air (n = 1), and the background material in yellow is silver. The permittivity of silver is characterized by Drude model $\varepsilon(\omega) = 1-\omega_p^2/(\omega^2 + i\omega\gamma_p)$, with $\omega_p = 1.38 \times 10^{16}$ Hz and $\gamma_p = 2.73 \times 10^{13}$ Hz. These parameters are obtained by fitting the experimental results [23].

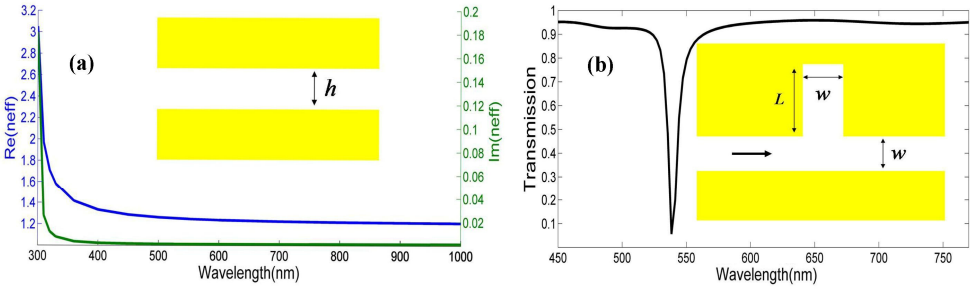

Fig. 1. (a) Blue and green curves represent the real and imaginary parts of the effective index n_{eff} of SPPs mode in ~~MDM waveguide~~ with width h = 100 nm, respectively. (b) Transmission spectra for MDM waveguide coupled to one stub, with w equaling to 100 nm and L being 500 nm. In both figures, insets display the corresponding schematic figures.

Figure 1(b) shows the transmission spectra for the MDM waveguide with one stub resonator. The inset in Fig. 1(b) displays the schematic of the system. The FDTD method and perfectly matched layer boundary conditions are used in the numerical experiment. From the CMT [24,25], the transmission of the system supporting a resonant mode of frequency ω_0 can be expressed as

$$T = \frac{(\omega-\omega_0)^2 + \left(\frac{1}{\tau_0}\right)^2}{(\omega-\omega_0)^2 + \left(\frac{1}{\tau_0}+\frac{1}{\tau_e}\right)^2}. \quad (1)$$

Here ω is the input frequency, $1/\tau_0$ and $1/\tau_e$ are the decay rate due to the intrinsic loss and the power escaping into the waveguide, respectively. It is obvious that the minimum transmission T_{min} at $\omega = \omega_0$ is determined by $1/\tau_0$ and $1/\tau_e$. When silver is replaced by the perfect electric conductor, $T_{min} = 0$. If there are two stub resonators side-coupled to MDM waveguide and the inter-space between them is adjusted gradually, what will happen to the transmission spectra?

#179233 - $15.00 USD Received 6 Nov 2012; revised 15 Mar 2013; accepted 26 Mar 2013; published 8 Apr 2013

3. Plasmon-induced-transparency with two stub resonators

3.1 Plasmon-induced transparency by direct coupling

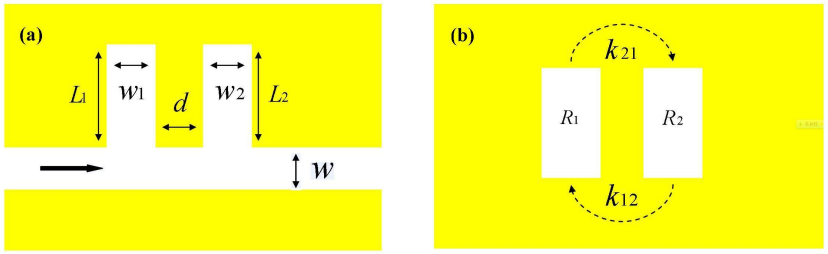

Fig. 2. (a) Schematic of MDM waveguide coupled to two stub resonators: w, the width of the waveguide; w_1 and w_2, the widths of the stub resonators; L_1 and L_2, the stub depths; d, the inter-space between the two stub resonators. (b) Illustration of direct coupling between two resonators denoted by R_1 and R_2. k_{12} and k_{21} are coupling coefficients.

Figure 2(a) is a schematic illustration of MDM waveguide coupled to two stub resonators. When d is small, the direct and indirect couplings coexist between the two stub resonators, but the indirect coupling does not have obvious influence on the resonant frequencies of the coupled system. So, we mainly consider the direct coupling, as shown in Fig. 2(b). Using the CMT [24,25], the energy amplitudes a_1 and a_2 for the resonators of resonant frequencies ω_1 and ω_2 can be described by

$$\frac{da_1}{dt} = i\omega_1 a_1 - \frac{1}{\tau_0} a_1 + k_{12} a_2, \tag{2}$$

$$\frac{da_2}{dt} = i\omega_2 a_2 - \frac{1}{\tau_0} a_2 + k_{21} a_1. \tag{3}$$

Here k_{12} and k_{21} are coupling coefficients related to the inter-space, $1/\tau_0$ is the decay rate due to the intrinsic loss. As shown in Fig. 1(a), the imaginary part of the effective refractive index n_{eff} for SPPs is in the range of 0.001 – 0.003 at visible frequency. The corresponding propagation length L_{spp} of SPPs is in the range of 10 – 30 μm, so we assume $1/\tau_0 = 0$ for simplicity. Then, the resonant frequencies of the coupled system can be deduced as

$$\omega = \omega_{\pm} = \frac{\omega_1 + \omega_2}{2} \pm \sqrt{\left(\frac{\omega_1 - \omega_2}{2}\right)^2 + |k_{12}|^2} \equiv \frac{\omega_1 + \omega_2}{2} \pm \Omega_0. \tag{4}$$

When $\omega_1 = \omega_2$, the resonant frequency is split. The frequency difference between the coupled modes is $\Delta\omega = 2\Omega_0 = 2|k_{12}|$, which is the transparent bandwidth mentioned in the latter section.

Based on Eqs. (1) and (4), we investigate the EIT-like transmission characteristics of MDM waveguide coupled to two stub resonators. Figure 3(a) represents the transmission spectra for the structure in Fig. 2(a) at different inter-spaces d, while the other parameters are set as $w = w_1 = w_2 = 100$ nm, and $L_1 = L_2 = 500$ nm. The transmission dips correspond to the resonant frequencies (ω_+ and ω_-) of the coupled system. When d is greater than 100 nm, the direct coupling between the two identical resonators is weak, and the resonant frequency ω_+ is approximately equal to ω_-, so the EIT-like responses do not appear. As d decreases from 100 nm, the transparent window presents and becomes increasingly evident, which is due to the increment of coupling coefficient between the two stub resonance modes and is in accordance with the CMT.

#179233 - $15.00 USD Received 6 Nov 2012; revised 15 Mar 2013; accepted 26 Mar 2013; published 8 Apr 2013

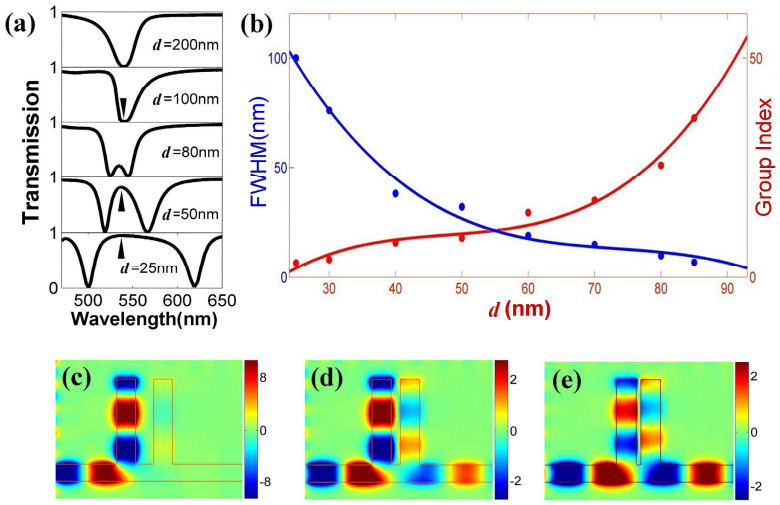

Fig. 3. (a) Transmission spectra of MDM waveguide coupled to two stub resonators at different inter-spaces d. (b) The FWHM and group index of the transparent window versus d. (c-e) Magnetic field distributions at three wavelengths marked by triangles corresponding to d = 100nm, 50 nm, and 25 nm, respectively. The other parameters are changeless, namely, w = w_1 = w_2 = 100 nm, L_1 = L_2 = 500 nm.

The measured full width at half maximum (FWHM) of the transparent window shown in Fig. 3(a) extends from 4 nm to 100 nm as d changes from 95 nm to 25 nm (plotted by blue dots in Fig. 3(b)). The corresponding group index of the transparent window for different inter-spaces d (plotted by red dots in Fig. 3(b)) can be approximately evaluated from the relation $n_g = \lambda^2/(4t\Delta\lambda)$ [26], where t is the propagation length in waveguide and $\Delta\lambda$ is the FWHM of the transparent window. Combining Fig. 3(a) and Fig. 3(b), we can see that there is a trade-off between transmission ratio and group index. The largest group index of ~61 associated with a group velocity of $v_g \approx 0.0164c$ is achieved when d = 95 nm, which is promising for the development of ultra-compact optical buffers. Such a system comprised of MDM waveguide side-coupled to a periodic array of the two direct coupling stub resonators can also be used to obtain slow light [12].

To get more insight into the physics of the observed EIT-like transmission, Figs. 3(c)-3(e) show the magnetic field distributions corresponding to three characteristic wavelengths marked by triangles for d = 100 nm, 50 nm and 25 nm, respectively. The magnetic field distributions indicate that the destructive interference of electromagnetic fields from the two resonators results in the EIT-like optical responses, which is similar to what happens in metamaterial-induced transparency. As d = 100 nm in Fig. 3(c), the stub on the right seems to make no difference, but the quality factor at resonant wavelength λ = 540 nm is smaller than that in Fig. 1(b), which is attributed to the increase of intrinsic loss.

#179233 - $15.00 USD Received 6 Nov 2012; revised 15 Mar 2013; accepted 26 Mar 2013; published 8 Apr 2013

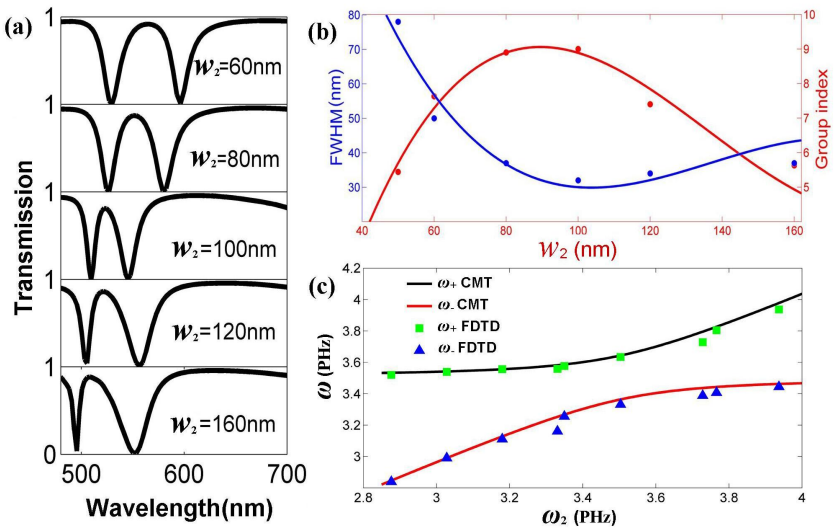

Fig. 4. (a) Transmission spectra of the structure shown in Fig. 2(a) for different w_2, and the other parameters are set as follows: $w = w_1 = 100$ nm, $d = 50$ nm, and $L_1 = L_2 = 500$ nm. (b) The FWHM and group index of the transparent window versus w_2. (c) Resonant frequencies (ω_+ and ω_-) of the system calculated using the CMT (solid curves) and FDTD method (dots).

In Fig. 4(a), we plot the transmission spectra for the system shown in Fig. 2(a), as $w = w_1 = 100$ nm, $d = 50$ nm, $L_1 = L_2 = 500$ nm, and $w_2 = 60$, 80, 100, 120, 160 and 170 nm, respectively. Figure 4(b) shows the FWHM and group index of the transparent window in Fig. 4(a). The FWHM (group index) of the transparent window decreases (increases) when w_2 varies from 40 nm to 100 nm, and then increases (decreases) as w_2 expands in the range of 100 – 160 nm. Consequently, for a fixed coupling distance in the direct coupling case, decreasing the difference between the two stub resonators gives rise to more pronounced slow-light effect. Comparing Fig. 3(b) with Fig. 4(b), we also find that the FWHM and group index to the inter-space between the two stub resonators are more sensitive than to the width of one cut, which provides an effective guidance for realizing the EIT-like phenomena. Figure 4(c) shows resonant frequencies (ω_+ and ω_-) of the system versus ω_2 using the CMT (solid curves) and FDTD method (dots). ω_2 is the resonant frequency of individual stub resonator and the other is $\omega_1 = 3.575$ PHz. We adjust ω_2 by w_2 and have $k_{12} = k_{21} = 1.4 \times 10^{14}$ Hz. With the increment of ω_2 from 2.8 PHz to 4 PHz, resonant frequencies (ω_+ and ω_-) of the system exhibit a blue-shift. The resonant frequency difference $\Delta\omega$ increases first and then decreases, which gives rise to the variation of transparent window in Fig. 4(a). As mentioned above, the formation and evolution mechanisms of plasmon-induced transparency by direct coupling have been proposed and accurately analyzed by the CMT, which is a powerful tool for the design of EIT-like systems.

3.2 Plasmon-induced transparency by indirect coupling

In this part, we introduce the indirect coupling scheme shown in Fig. 2(a) by referring to [17,21]. The parameter d is tunable and large enough that the two stub resonators do not interact with each other directly. All the other parameters of the structure are set as follows: $w = w_1 = w_2 = 100$ nm, $L_1 = 500$ nm, $L_2 = 480$ nm. Figure 5(a) shows the transmission spectra for different inter-spaces d. The curves with circles and triangles are the transmission spectra of the system with individual stub resonator (shown in Fig. 1(b)) comprising the coupled system. As expected, the transparent band is between the two individual stub resonator resonances. Moreover, the transparent resonance peak exhibits a shift and its symmetry is tunable.

#179233 - $15.00 USD Received 6 Nov 2012; revised 15 Mar 2013; accepted 26 Mar 2013; published 8 Apr 2013

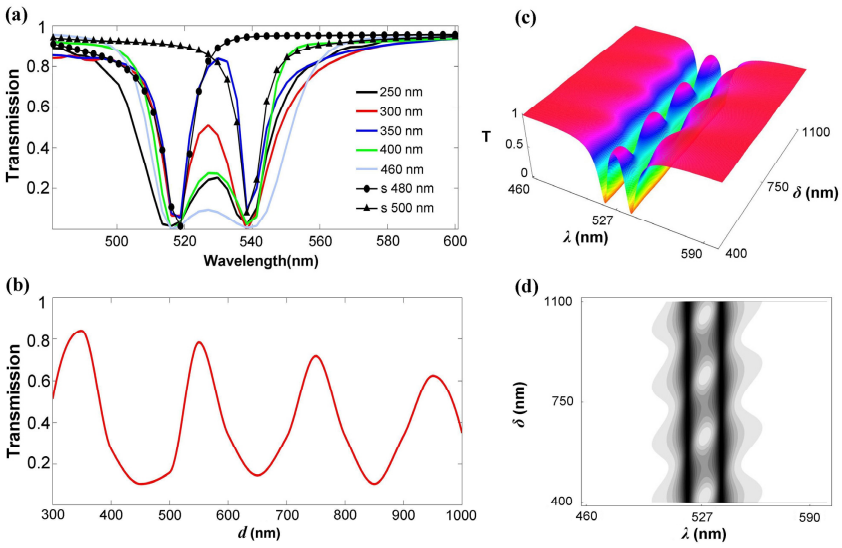

Fig. 5. (a) Transmission spectra of MDM waveguide coupled to two stub resonators at different inter-spaces d with $w = w_1 = w_2 = 100$ nm, $L_1 = 500$ nm, $L_2 = 480$ nm. The curve with circles is transmission spectra for the one stub system (shown in Fig. 1(b)) with $w = 100$ nm, $L = 480$ nm, and the curve with triangles corresponds to the one stub system with $w = 100$ nm, $L = 500$ nm. (b) Transmission spectra for different inter-spaces d at $\lambda = 527$ nm. (c) Evolution of the transmission spectra versus δ and λ. (d) The top view of Fig. 5(c).

The spacing dependence of the transparent window indicates the indirect coupling system as a two-mirror FP resonator [17, 21], in which the waveguide region between the two stub resonators acts as a FP cavity. The transmittance of the indirect coupled system can be given as

$$T(\omega) = \left| \frac{t_1(\omega)t_2(\omega)}{1 - r_1(\omega)r_2(\omega)e^{i2\beta(\omega)\delta}} \right|^2, \tag{5}$$

namely

$$T(\omega) = \left(\frac{|t_1(\omega)t_2(\omega)|}{1 - |r_1(\omega)r_2(\omega)|} \right)^2 \frac{1}{1 + 4\left(\frac{\sqrt{|r_1(\omega)r_2(\omega)|}}{1 - |r_1(\omega)r_2(\omega)|} \right)^2 \sin^2\theta}, \tag{6}$$

where $\theta = Arg[r_1 r_2 \exp(i2\beta\delta)]/2$ is one-half of the round trip phase in the FP cavity. $\beta(\omega) = \omega n_{eff}/c$ is the propagation constant for SPPs between two resonators. $t_j(\omega) = [i(\omega_j - \omega) + \omega_j/(2Q_{oj})]/[i(\omega_j - \omega) + \omega_j/(2Q_{oj}) + \omega_j/(2Q_{ej})]$ and $r_j(\omega) = -[\omega_j/(2Q_{ej})]/[i(\omega_j - \omega) + \omega_j/(2Q_{oj}) + \omega_j/(2Q_{ej})]$ ($j = 1, 2$) are frequency-dependent transmission and reflection coefficients of the two mirrors with separation δ, and Q_{oj} (Q_{ej}) stands for intrinsic (coupling) quality of the jth stub resonator.

From Fig. 1(a) and Eq. (6), we can obtain that Re(n_{eff}) (the real part of the effective index of SPPs) approximately equals 1.254 and the periodicity of transmittance is 210 nm for $\lambda = 527$ nm. Using the FDTD simulations, we plot the transmission spectra in Fig. 5(b), in which the transmittance at $\lambda = 527$ nm varies periodically and the periodicity is 200 nm approximately. The slight difference in the periodicity between the FP model and FDTD method is caused by the inaccuracy of the propagation constant or the finite mirror size in the structure. The maximum of transmission spectra at $\lambda = 527$ nm gradually becomes smaller,

#179233 - $15.00 USD Received 6 Nov 2012; revised 15 Mar 2013; accepted 26 Mar 2013; published 8 Apr 2013

which is due to the increase of the intrinsic loss. It is also noteworthy that the peak (dip) transmission at λ = 527 nm corresponds to phase retardation condition $\beta\delta = N\pi$ ($\beta\delta = (N + 1/2)\pi$), for which the magnetic field distributions (not shown here) are consistent with [21] and N is an integer.

In Fig. 5(a), the resonant wavelengths for the two individual stub resonators are λ = 538.4 nm and 518.7 nm, respectively. $Q_t = \lambda_0/\Delta\lambda$ represents the total quality of the side-coupled stub resonator ($1/Q_t = 1/Q_o + 1/Q_e$), where λ_0 and $\Delta\lambda$ are the peak wavelength and the FWHM of the reflection spectrum. The intrinsic quality factor Q_o of the sub resonator can be estimated from [17]. So, in this structure, $Q_{o,j}$ (j = 1,2) are about 500. $Q_{t,1}$ and $Q_{t,2}$ are about 63 and 61, respectively. Thus, $Q_{e,1}$ is about 72 and $Q_{e,2}$ is about 69.5. To further clarify the transmission characteristics, the transmission spectra versus δ and λ are shown in Fig. 5(c). Because of the finite mirror size in the structure, we set approximately $\delta = (d + 100)$ nm. It is found that the EIT-like transmittance varies periodically versus δ. For a determined δ, the transmission spectra agree well with that of Fig. 5(a). To exhibit more explicitly the formation and evolution mechanisms of plasmon-induced transparency by indirect coupling, we show in Fig. 5(d) the top view of Fig. 5(c). Dark (light) represents low (high) transmittance. As δ changes (resulting in the change of $\sin^2\theta$ in Eq. (6)), the transparency peak exhibits a shift and the symmetry of which also changes, while the transmission dips corresponding to resonant cavity modes remain unchanged. Consequently, for the case of plasmon-induced transparency by indirect coupling, the formation of transparency window is determined by the resonance detuning and the evolution of the transparency is mainly attributed to the change of coupling distance.

4. Conclusion

In summary, we have numerically and theoretically explored EIT-like spectral responses in plasmonic system composed of two sub resonators side-coupled to MDM waveguide. The results show that both the direct and indirect couplings between the two stub resonators lead to plasmon-induced transparency. For the directly coupled case, the EIT-like spectral response can be manipulated by adjusting the coupling distance and resonance detuning, which can be interpreted by the CMT. Decreasing the difference between the two stub resonators with fixed coupling distance gives rise to more pronounced slow-light effect. Moreover, the FWHM and group index of the transparent window to the inter-space are more sensitive than to the width of one cut, and the high group index of up to 60 can be achieved at visible frequency. For the case of only indirect coupling, the formation of transparency window is determined by the resonance detuning and the evolution of the transparency is mainly attributed to the change of coupling distance, which can be accurately analyzed by the FP model. Both the CMT and FP model agree well with the FDTD simulations. Hence, the plasmonic waveguide system may have potential applications for nanoscale optical switching, plasmonic sensing, and slow-light devices in highly integrated optical circuits.

Acknowledgments

This work was funded by the Fundamental Research Funds for the Central Universities of Central South University under Grant No. 2012zzts007, the Research Fund for the Doctoral Program of Higher Education of China under Grant No. 20100162110068, and the National Natural Science Foundations of China (Grant No. 61275174 and 11164007).